A comparative study of the anticorrosive response of *Tinospora cordifolia* stem extract for Al and Cu in biodiesel-based fuels

Kumar Amgain[1], *Bhesh Nath* Subedi[1], *Susan* Joshi[1], and *Jagadeesh* Bhattarai[1,*]

[1]Central Department of Chemistry, Tribhuvan University, Kirtipur 44619, Nepal

Abstract. The anticorrosive effect of methanol extract of *Tinospora cordifolia* stem for Al and Cu metals in pure biodiesel and its 10% blend with petrodiesel was investigated at 25±2 °C in a closed system by corrosion, inhibition efficiency, adsorption, and electrochemical tests. The corrosion inhibiting action of the plant extract for Cu in the biodiesel was more efficient than in the blend, while the extract showed more anticorrosive behavior of Al metal in the blend than in the biodiesel. Adsorption of the plant extract on the metal surface conformed to the Langmuir adsorption model. The plant extract functioned as a mixed-type corrosion inhibitor for both the metals in both biodiesel and its blend based on the experimental results. Outcomes of the study confirm the suggestive evidence to formulate the green extract-based biodiesel additives to enhance the anti-corrosive response for the Al and Cu metal parts of the vehicle engine. Nepal-origin *Tinospora cordifolia* stem extract could be used as an anticorrosive agent to control the corrosion of Al and Cu metals in biodiesel-based fuels.

Keyword. Biodiesel, Corrosion inhibitor, Immersion test, Plant extract, Polarization

1 Introduction

The European countries put forwarded rules of the renewable energy directive II for targeting to share at least 32% biofuels in the transport system by 2030 [1]. Biodiesel and its blends are one sort of biofuel, which are proven alternative renewable fuel that substitutes petroleum diesel. Because biodiesel-based fuels (BDBFs) have close properties with petroleum diesel [2]. They are eco-friendly [3, 4], and perform almost the same behavior as that of non-renewable petroleum fuels [5]. The utilization of such greener biodiesel-based fuels in vehicle engines becomes advantageous because they significantly diminish the toxic gas emissions, and are biodegradable, economical sources of renewable energy [6]. The BDBFs produce about 4.5 times of energy units than the counter fossil fuels [7] and have shown superlubricity behavior [8].

Biodiesel has been mandated for its usage in a blending range of up to 20% with petroleum diesel all over the world [9], although there are some challenges to making such greener BDBFs into reality. In comparison to petroleum diesel, the BDBFs are more corrosive to the engine parts of transportation means and the fuel storage systems [10, 11], which are mostly fabricated by steel, cast iron, aluminum, copper so on [12]. There is a growing trend to replace steel and cast iron with Al and Cu metals, and their alloys in vehicle engines and fuel storage systems in recent decades [13].

Excellent mechanical properties, good corrosion resistance, and adequate ductility of high-strength Al alloys led to significant attention in various industrial sectors [14], including aviation and automotive industries to replace steel components with much lighter parts of aluminum-based materials [15]. The Al and its alloys are usually utilized in different parts of the vehicle engine like pistons, cylinder heads, and engine blocks [16], whereas pumps, injectors, starters, ignition coils, and heat exchangers are made of Cu and its alloys [17].

The anti-corrosive nature of petroleum diesel decreases by increasing the biodiesel concentration in the BDBFs, mostly due to fostering microorganism activities in the biodiesel fuels [18]. Besides, researchers corroborated that the BDBFs reported more corrosive than the petroleum diesel on uncoated gray cast iron [19], and AA 3003 aluminum meal [20], mostly due to a marked increase in water, total acidity, electrical conductivity, density, and viscosity so on of the BDBF as compared to the petroleum diesel after immersion tests. From the electrochemical tests, the corrosion-resistance of carbon steel was reported the highest (at least one order of magnitude) in comparison to Al as well as the Cu in biodiesel, and the Cu metal showed the lowest corrosion-resistant properties than carbon steel and Al metals in biodiesel [21]. In most cases, the blending of biodiesel with 80% petroleum diesel or more has been practiced to improve its physical, chemical, and anticorrosive properties [22].

For the last decades, it becomes one of the effective techniques for minimizing the corrosion rates of different structural materials by mixing sufficient amounts of plant-based green inhibitors in aggressive electrolytes [23-25], except biofuels. Few studies demonstrated that biodiesel and its blends with a small addition of the plant-based green extracts have sufficient capability and possibilities to inhibit the corrosion

* Corresponding author: bhattarai_05@yahoo.com

problems of metals in the biofuels [26, 27]. One more research step is projected in this study to perform the anticorrosive response of methanol extract of *Tinospora cordifolia* stem (METcS) as a green inhibitor in pure biodiesel (BD-100) and its 10% blend (BDB-10) to control the corrosive nature of these biofuels towards Al and Cu metals using the immersion and electrochemical tests.

Tinospora cordifolia (known as GURJO in Nepali and heart-leaved moonseed in English), belonging to the Menispermaceae family, is one of the largest deciduous climbing shrubs and is distributed throughout Nepal, including other South Asian countries. It is used in folk and the Ayurvedic system of medicine by the local people of Nepal [28]. The stem extract of the Nepal-origin *T. cordifolia* plant reported various secondary plant metabolites like alkaloids, glycosides, coumarins, triterpenes, phenols, saponins, and tannins based on the phytochemical screening tests only [29]. The presence of the phytomolecules having O, N, S heteroatoms, multiple bonds, and aromatic ring compounds of the METcS will act as efficient green-based additives in different biofuels, such as biodiesel-based fuels (BDBF), to enhance the anticorrosive response to the aluminum, copper and their alloys.

However, it has not been reported so far the important aspects of this plant species as a corrosion inhibitor source to extend the lifetime and corrosion-resistant behavior of different automotive engine metals in the BDBF, although very few studies have been reported the corrosion inhibiting efficacy of *T. cordifolia* [30, 31], and *T. crispa* [32] extracts for steel in acidic electrolytes. In such conditions, the main goal of this study is to explore the METcS as green inhibiting additives to the BD-100 and BDB-10 fuels on a commercial scale to control their corrosive nature towards Al and Cu metals. The output of the experimental results would be helpful to manufacturers and policymakers for the mass production of automotive engine benign biodiesel and its blend fuels in Nepal.

2 Materials and methods

A rectangular-shaped (i.e., 4 cm × 3 cm × 0.4 cm) Al and Cu plats were mechanically polished to make a mirror shine surface, using 200-1500 grit numbers SiC paper in ethanol, rinsed by acetone, and air-dried to obtain consistent results from immersion, inhibition and electrochemical tests. The test electrolytes to accomplish this research were pure biodiesel (BD-100), which was produced at a laboratory scale from a cooked-oil residue (COR) as per the trans-esterification method, as described elsewhere [33]. Besides, a 10% blend (BDB-10) of the biodiesel with commercially available petroleum diesel (PetD) was also prepared. Then, some physical properties of the BD-100 synthesized from the COR were assessed using ASTM standards and compared with the properties of the PetD. Besides, gas chromatographic (GC), and FTIR spectroscopic techniques were carried out using instruments of a GC-2010 model (Shimadzu, Japan) and IRTacer-100 model (Shimadzu, Japan), respectively, for the quality analysis of both the BD-100 and PetD.

The METcS extract from stem powder of the *T. cordifolia* plant was acquired by soxhlet extraction using the rotatory evaporation technique, as explained elsewhere [34]. Then, the methanol extract was dried and stored at 4 °C before its use as biofuel additives. The dried solid plant extract obtained was named the METcS. The required amount of the stored METcS was weighted and added in both BD-100 and BDB-10 fuels separately to prepare their 500, 1000, 1500, and 2000 ppm electrolytic solutions.

The weight lost (Δw) of each Al and Cu specimen after immersion time (t) in the BD-100 and BDB-10 electrolytes without and with METcS concentrations was used for estimating their corrosion rate (CR) using a formula, as depicted in equation (1), where Fc (= 87600) is a conversion factor [35]. Also, the CR of both metals in a commercially available PetD was estimated for comparative study.

After the estimation of the CR of each Al or Cu specimen in different test biofuels without and with the METcS, the degree of surface coverage (θ) and % corrosion inhibition efficiency ($CIE_{\%}$) were calculated using equations (2) and (3), respectively [36]. The authors assumed herein the calculated θ is based on the METcS entirely controls the dissolution of Al or Cu from the covered surfaces [37].

$$CR\,(mm/yr) = \frac{Fc \times \Delta w\,(g)}{\text{area}\ (cm^2) \times \text{density}\ (g/cm^3) \times t\,(hr)} \quad (1)$$

$$\theta = \frac{CR_{without} - CR_{with\ METcS}}{CR_{without}} \quad (2)$$

$$CIE_{\%} = \frac{CR_{without} - CR_{with\ METcS}}{CR_{without}} \times 100 \quad (3)$$

Besides, the protective layer formation mechanism on the corroded Al and Cu surfaces after exposing these metals in BDBF electrolytes with the METcS was investigated using Langmuir and Temkin adsorption isotherm models. The inhibiting action of the METcS to the corroded Al and Cu metals was explained from the calculated adsorption equilibrium constant (K_{ads}) using the Langmuir adsorption model [38], as given in equation (4), where the C_{METcS} is the used concentration of the METcS.

In addition, the Temkin adsorption model [39] could be used to explain the adsorption mechanism of inhibition action of phytomolecules of the METcS onto the corroded metal surfaces, as shown in equation (5). In equation (5), the Temkin equilibrium constant (K_T) and constant B (= $RT/\Delta H_{ads}$) provide the information about binding energy, and change of heat (ΔH_{ads}) for an adsorption experiment, respectively [40]. The graphical plot of θ aginst $\log C_{METcS}$ shows a line that obeys the Temkin adsorption model [39].

$$\frac{C_{METcS}}{\theta} = \frac{1}{K_{ads}} + C_{METcS} \quad (4)$$

$$\theta = B \log K_T + B \log C_{METcS} \quad (5)$$

The anodic polarization curve was recorded from the rest of the potential value observed after a half-hour immersion to understand the passivity and electrochemical behavior of Al and Cu metals in both the BD-100 and BDB-10 biofuels containing different concentrations of the METcS at 25±2 °C, as elucidated in the previous work [41]. For this purpose, a potentiostat/galvanostat (Hokuto Denki HA-151, Japan) was used by adjusting the 15 mV/min scan rate. Before the electrochemical measurements, about 0.1 g/L $LiClO_4$ supporting electrolyte was added to each BD-100 and BDB-10 test electrolyte to increase their conductivity, as described elsewhere [42]. A saturated $Hg/Hg_2Cl_2/Pt$, Al or Cu coupon, and graphite rod were used as a reference, working, and auxiliary electrodes, respectively.

3 Results and discussion

The experimental data on the physical properties of the cooked-oil residue (COR) biodiesel are found within the limits of the ASTM D6751-14 standard of commercial biodiesel [43], as summarized in Table 1. Based on the observed physical properties, virtually pure and contamination-free biodiesel (i.e., BD-100) was successfully synthesized from the COR using transesterification. Hence, the BD-100 and its bend could be used in a diesel engine as a renewable biofuel by improving its corrosive response.

Table 1. Physical properties of the COR biodiesel.

Properties	COR biodiesel	Commercial biodiesel [43]
Appearance	Yellow	Yellow
Odor	Mild	–
Water and sediment (%)	Trace	0.05
Physical state	Liquid	Liquid
Boiling point (°C)	234	182-338
Kinematic viscosity (mm^2/s)	4.94	1.9 to 6.00
Specific gravity at 25 °C	0.91	0.86 to 0.90

Furthermore, the quality analysis of the BD-100 and its blend becomes important for their successful use as a surrogate of petroleum diesel on a commercial scale. From the qualitative GC analysis, six peaks were recorded in the chromatogram of the COR biodiesel (not shown), and their percentage area, retention time, and name of the FAMEs are listed (Table 2), based on the library search report. No other peaks except the six peaks of the FAME were observed in the Gas Chromatography (GC), indicating the absence of the byproducts like glycerol and other impurities in the synthesized COR biodiesel.

Table 2. Lists of the constituents of the COR biodiesel identified from the gas chromatograph.

Rt* (min.)	Area (%)	Name of FAMEs
52.86	8.92	Hexadecanoic acid methyl ester
58.19	50.93	9,12-Octadecadienoic acid methyl ester
58.38	33.84	11-Octadecenoic acid methyl ester
58.51	1.39	16-Octadecenoic acid methyl ester
58.58	1.19	9-Octadecenoic acid methyl ester
59.11	3.73	Cyclopentanetridecanoic acid methyl ester

**Retention time*

However, only the GC is not an adequate method for the characterization of the biodiesel blend with petroleum diesel, mostly due to the jeopardy of the overlapping signals of the complex spectra of long chains of petroleum carbon [44]. Thus, the FTIR spectroscopic method becomes more relevant to evaluate the FAME contents and quality of the biodiesel and its blends. The results of the non-existence of broadband around the 3100-3500 cm^{-1} region confirmed the absence of moisture, free fatty acid, and even glycerol in the synthesized COR biodiesel (Table 3). Three FTIR peaks in the 3008-2853 cm^{-1} range can be credited to the stretching vibration of the C–H bonds of the $-CH_2$ group, which are in agreement with the FTIR of edible oil [45].

Table 3. Comparative discussion of the FTIR spectra between the synthesized biodiesel and its raw cooked-oil residue.

Cooked-oil Residue (COR)		*COR Biodiesel (BD-100)*	
Vibration (cm^{-1})	Spectral assignment	Vibration (cm^{-1})	Spectral assignment
3008	C−H stretching; C=CH_2	3008	C−H stretching; C=CH_2
2923	C−H asymmetrical stretching; −CH_2	2923	C−H asymmetrical stretching; −CH_2
2853	C−H symmetrical stretching; −CH_2	2853	C−H symmetrical stretching; −CH_2
1744	C=O stretching; ester	1741	C=O stretching; –OCH_3
1460	C−H bending; −CH_2	1458	C−H bending; −CH_2
–		1435	Deformation vibration, –OCH_3
1377	C−H bending; −CH_2	1366	C−H bending; −OCH_3 (biodiesel)
1236	C−H bending; −CH_3	1229	C−O stretching of a typical ester
–		1215	C−O stretching; −OCH_3
–		1205	C−O stretching; FAMEs
–		1169	C−O stretching; FAMEs
1159	C−O stretching; C−O−C (Average)	–	
1097		–	
1032	C−O stretching; ester	1020	C=O bending; –OCH_3
968	C−H deformation; unsaturated fatty acid	–	
–		880	
721	C−H rock bending; $(-CH_2)_n$, n≥4	721	C−H rock bending; $(-CH_2)_n$, n≥4

It demonstrated the strongest peak at 1744 cm^{-1} among all the others absorption bands of the specimen, which is the characteristic of the ester C=O stretching vibration. However, a shifting of the peak to 1741 cm^{-1} with strong absorption intensity was ascribed to the C=O group of the methyl ester (Table 3). The C=O stretch of the ester absorbs light at 1740±5 cm^{-1} in the FTIR spectra, which is employed in the analysis of biodiesel content as the peak maximum [46].

Biodiesel has several characteristic FTIR absorption bands at 1435 cm^{-1}, 1365 cm^{-1}, and multiple peaks in the 1229-1169 cm^{-1} range [47]. A narrow absorption band of 1435 cm^{-1} moves along from the 1460 cm^{-1} of the raw cooking oil. The band at 1435 cm^{-1} was contemplated to the deformational vibration of the $-OCH_3$ group of the biodiesel. The band at 1377 cm^{-1} was attributed to the O-CH_2 of the raw COR, and this band was diminished with appearing as a strong band at 1366 cm^{-1} in the spectra of the COR biodiesel (Table 3), mostly due to the C−H bending vibration of O−CH_3 group.

The average energy of the triglycerides is no longer present at 1159 cm^{-1} after the synthesis of biodiesel from the raw COR, and this band was separated into multiple peaks in the region between 1229-1169 cm^{-1}. They assign to the C−O stretching and bending of the $-OCH_3$ group of the COR biodiesel. Very weak bands at 1032 cm^{-1} and 968 cm^{-1} were observed in the raw COR, which may be due to the C-O stretching vibrations, and the C-H out-of-plane deformation of unsaturated fatty acids, respectively [48], which disappeared in the biodiesel sample. The 721 cm^{-1} band in both the raw COR and synthesized biodiesel samples remarked to rock-bending vibration of the $(–CH_2)_n$ groups for $n \geq 4$, as ascribed elsewhere [47]. The summaries of these FTIR peak assignments are condensed in Table 3.

The corrosive response of two biodiesel-based biofuels (i.e., BD-100 and BDB-10), including PetD fossil fuel to Al and Cu metals is described from the estimated CR of the metals after immersion for about 16-189 days in 3 types of vehicle fuels at 25±2 °C, and the results are summed up in Table 4. It is easy to perceive from the tabulated data that both metals showed a lower CR in PetD than BD-100. Such corrosion behavior was reported more or less in the literature for the Al, Cu, cast iron, and carbon steel in palm biodiesel [49], partially due to increasing the total acid number (TAN) values of the biodiesel at the end of immersion for four months [50].

A unique elemental dissimilarity between the BDBFs and PetD is due to the presence of oxygen atoms in the biofuels, which make them more polar and able to create hydrogen bonds with water. This property of the BDBFs enhanced to increase the corrosion rate of metals than in the PetD. Besides, the blending of the biodiesel with petroleum diesel decreases the anticorrosive response to Cu metal, although an anomalous corrosion trend is observed for Al metal in BDB-10.

Table 4. The corrosion rate of Al and Cu metals in the BDBFs, including the PetD at 25±2 °C in a closed vessel at different periods.

Immersion time	CR of Al metal (mm/yr) in			CR of Cu metal (mm/yr) in		
(hr)	*BD-100*	*BDB-10*	*PetD*	*BD-100*	*BDB-10*	*PetD*
384	0.00697	0.00216	0.00291	0.00787	0.00330	0.00068
768	0.00531	0.00208	0.00301	0.00793	0.00334	0.00074
1536	0.00287	0.00155	0.00159	0.00799	0.00316	0.00065
2184	0.00228	0.00156	0.00138	0.00907	0.00331	0.00054
2976	0.00191	0.00117	0.00113	0.01121	0.00352	0.00055
4520	0.00104	0.00101	0.00089	0.01021	0.00334	0.00042

A high corrosive level of biodiesel (BD-100) to Cu should be due to low oxidative stability in comparison to Al, which is also in agreement with the earlier outcomes [51]. The oxidative stability determines the fuel quality and essentially influences the biodiesel stability [22]. It is reported that the addition of plant-based natural anti-oxidative phytomolecules in biodiesel and its blends enhanced their oxidative stability for long period uses or storage in vehicle engines [52]. The CR of the Al metal in the BDB-10 is slightly lower than in PetD up to the initial 24 days of exposure, and it becomes almost the same until about 189 days of exposure. In this circumstance, it becomes a fascinating topic to perform experimental works for knowing the effectiveness of different concentrations of METcS to increase the anticorrosive response of Al and Cu metals in BD-100 and BDB-10 fuels.

For this purpose, the corrosion-resistant behavior of Al and Cu metals was studied in BD-100 and BDB-10 in the absence and presence of 500, 1000, 1500, or 2000 ppm METcS concentrations. The anticorrosive behavior of Al metal increased significantly (i.e., nearly one order of magnitude) by increasing the concentrations of the METcS in BD-100 and BDB-10 biofuels, as shown in Figure 1(a), and 1(b), respectively. However, the corrosive effect of the different concentrations of the plant extract in both the BD-100 and BDB-10 fuels to Cu metal seems to be different and is less than that of Al metal.

The corrosion rate of Cu in each BD-100 or BDB-10 fuel with 500 ppm METcS is lower than in other concentrations, which is slightly increased with increasing the concentrations of the METcS from 1000 ppm, although their corrosive nature to the Cu is lower than in BD-100 and BDB-10 without the extract, as shown in Figure 1(c) and 1(d), respectively. These results revealed two important findings; firstly the METcS could be used as a good green-based corrosion inhibitor to increase the corrosion resistance properties of different vehicular engine metals like Al and Cu in pure biodiesel (BD-100) obtained from the COR, and its blend (BDB-10) at 25 °C in a closed system. The addition of 500 ppm METcS in both the biofuels seems to be a sufficient concentration of the METcS to improve

* Corresponding author: bhattarai_05@yahoo.com

the corrosion-resistant properties of Cu in both the DBBFs at room temperature.

Besides, Table 5 shows the result of the calculated % corrosion inhibition efficiency ($CIE_{\%}$) of the METcS for Al and Cu metals in both the BDBFs (i.e., BD-100 and BDB-10) fuels. The $CIE_{\%}$ increases by increasing the METcS amounts (i.e., 1000-2000 ppm) in BDB-10 in the case of Al metal to maintain the optimal $CIE_{\%}$ (i.e., 86.1%), despite the additions of 1000-2000 ppm METcS in the BD-100 enhanced to increase the $CIE_{\%}$ slightly to attain the optimal value of about 78.8%.

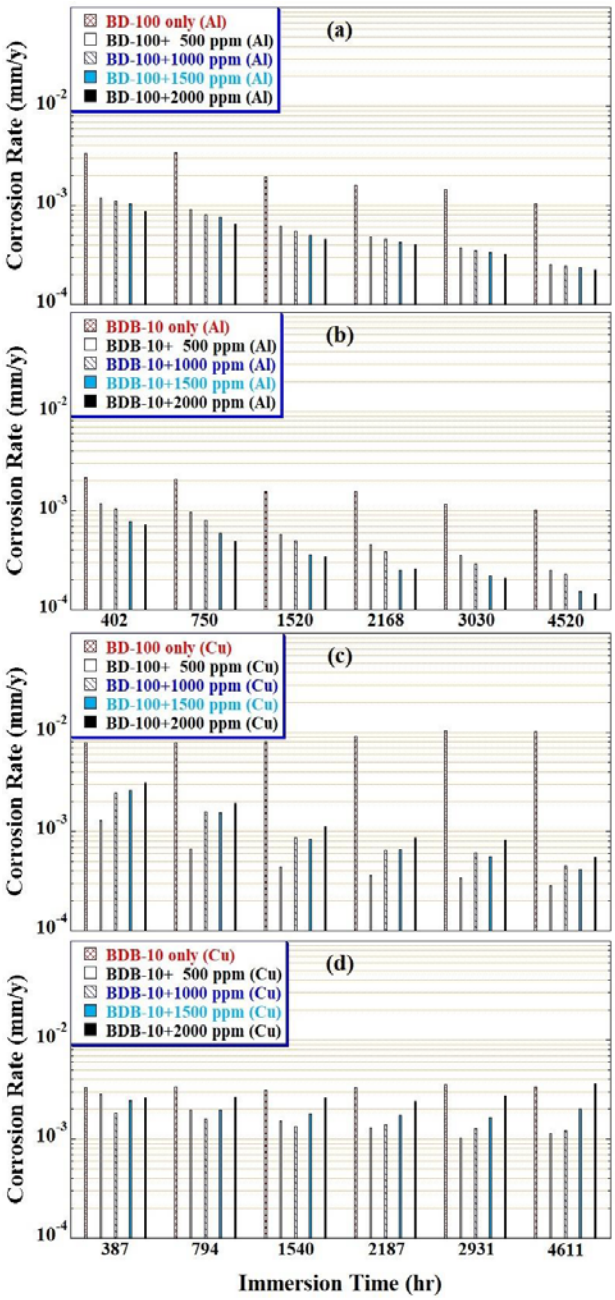

Figure 1. Effect of different concentrations of METcS on the corrosion rates of Al in (a) BD-100, (b) BDB-10, and Cu in (c) BD-100, and (d) BDB-10 at 25±2 °C and closed condition, against the exposure time.

In contrast, the $CIE_{\%}$ of 1000-2000 ppm extract in BD-100 fuel to Cu metal is decreased, and especially the decreasing trend of the $CIE_{\%}$ by increasing of 1000-2000 ppm METcS in the BDB-10 is significantly higher than in BD-100 for the Cu metal (Table 5). Consequently, the addition of 500 ppm METcS in BD-100 and BDB-10 shows the optimal $CIE_{\%}$ of about 97.3% and 66.2%, respectively, compared to Cu.

Results disclosed that the corrosion inhibition action on Cu metal significantly decreases with the addition of more than 500 ppm METcS in the B10. Such behavior of the significant acceleration of the corrosion rate of Cu metal in BDB-10 with the additions of 1000-2000 ppm METcS is more, probably due to the formation of an unstable surface film on Cu at a high amount of the METcS in BDB-10. At large, the corrosion inhibition study, based on the adsorption isotherm model, reported that the fractional surface coverage (θ) was increased by increasing the inhibitor amounts to a fixed optimal concentration, mostly due to the saturation of the corroded metal surface sites according to the adsorption model [53].

Overall, the order of the inhibiting efficiencies of METcS in both the BDBFs for Al and Cu metals could be arranged as; $CIE_{\%\ for\ Cu\ in\ BD\text{-}100+METcS} > CIE_{\%\ for\ Al\ in\ BDB\text{-}10+METcS} > CIE_{\%\ for\ Al\ in\ BD\text{-}100+METcS} > CIE_{\%\ for\ Cu\ in\ BDB\text{-}10+METcS}$. Therefore, the methanol fraction of the stem extract of *T. cordifolia* (i.e., METcS) would be efficient green-based materials for the formulation of the BDBF additives for controlling their corrosive nature to Al and Cu.

The Langmuir and Temkin adsorption models have been used to approximate the thermodynamic parameters to understand the adsorption mechanism of the corrosion inhibitors [54]. In the Langmuir model, the linear relationship between C_{METcS}/θ and C_{METcS} for Al and Cu metals in both the BDBFs with METcS concentration is displayed in Figure 2(a). Also, a linear form of the Temkin adsorption model was tested for comparative elucidation, as illustrated in Figure 2(b). The Langmuir adsorption model should be the best-fitted, based on the experimentally calculated linear correlation coefficient (R^2 ~1) and slope values (Figure 2a). However, the R^2 ranges from 0.8414 to 0.9748 for the Temkin equation.

These adsorption properties suggest the homogeneous distribution of adsorbed sites onto the corroded Al and Cu surfaces to form a corrosion-preventing monolayer film, although the Al metal in BD-100 shows a disparity in the Langmuir slope value. It deviates to some degree from the unity, which indicates that there is not a uniform explanation of the assumption of monolayer adsorption of the phytomolecules of the METcS onto the Al surface in BD-100. The Langmuir adsorption model suggested the interaction between the adsorbate and adsorbent, not between the adsorbate-adsorbate interactions [55]. A similar consequence was reported in the literature on the surface of mild steel specimens to control their corrosion in aggressive acids [56, 57].

Moreover, an endothermic type of the adsorption reaction enhances the formation of a protective passive film on the corroded Al surface in both BD-100 and BDB-10 biofuels, which is supported by the slope value (i.e., B>0) of the Temkin adsorption equation [58]. Such reaction mechanism obeyed to inhibit the corrosion of Al

in both the BDBFs with 500-2000 ppm METcS. However, the corrosion inhibiting the efficiency of Cu metal is decreased in BD-100 with more than 500 ppm METcS, mostly due to the existence of an exothermic type of adsorption reaction, which is not beneficial for further protection of the passive film of Cu metal in the presence of 1000-2000 ppm METcS in both the BDBFs. Such results from the Temkin model indicated that the intermediate concentration range of the METcS should be 500 ppm or less, not more than it for the corrosion control of Cu in the BDBFs.

Table 5. The corrosion rate (CR) and % corrosion inhibition efficiency ($CIE_{\%}$) of Al and Cu metals in the BD-100 and BDB-10 with different concentrations of the METcS at 25±2 °C in a closed system.

Concentration of METcS (ppm)	*Al metal in DBFs*				*Cu metal in BDBFs*			
	CR_{BD-100} (mm/y)	CIE_{BD-100} (%)	CR_{BDB-10} (mm/y)	CIE_{BDB-10} (%)	CR_{BD-100} (mm/y)	CIE_{BD-100} (%)	CR_{BDB-10} (mm/y)	CIE_{BDB-10} (%)
0	0.00104	–	0.00101	–	0.01021	–	0.00334	–
500	0.00026	75.0	0.00032	68.3	0.00028	**97.3**	0.00113	**66.2**
1000	0.00024	76.9	0.00023	77.2	0.00045	95.6	0.00121	63.8
1500	0.00023	77.9	0.00015	85.1	0.00042	95.9	0.00199	40.4
2000	0.00022	**78.8**	0.00014	**86.1**	0.00055	94.6	0.00359	-00.1

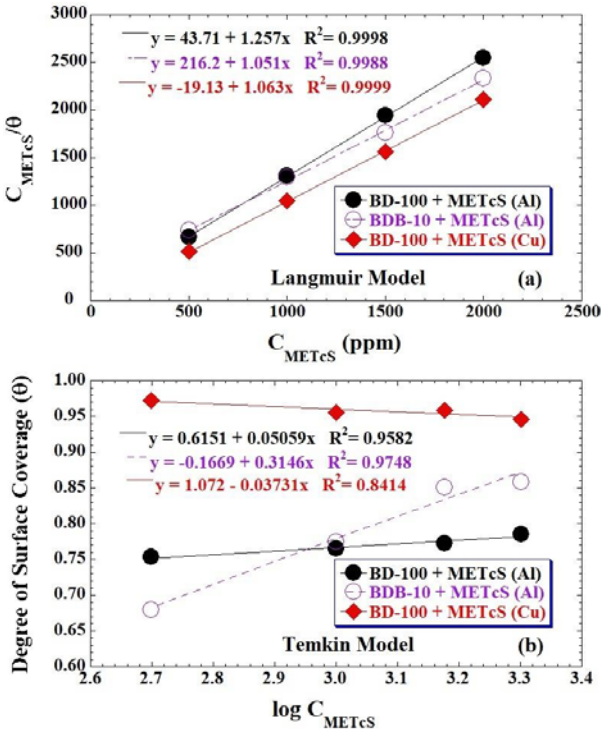

Figure 2. The Langmuir (a), and Temkin (b) adsorption isotherm plots for Al and Cu metals after exposure for 4520 h in both the BDBFs with different concentrations of METcS at 25±2 °C in a closed system.

Consequently, the corrosion-resistant of Cu decreased by increasing the METcS concentration, more than 500 ppm in both the BDBFs, as shown in Figure 1(c), and 1(d) also, although a high surface coverage (θ) is obtained for Cu metal in BD-100 with METcS than for Al in both the BD-100 and BDB-10 electrolytes (Table 5). In general, the Temkin adsorption isotherm model is assumed to be valid only at the intermediate concentration of adsorbate [59]. It reported a heterogeneous surface by which the adsorption heat changes (ΔH_{ads}) differ linearly from the θ by the adsorbate [60]. Consequently, the estimated ΔH_{ads} is decreased linearly with increasing the θ (Figure 2b).

The main purpose of the METcS addition in BDBFs is to increase the anticorrosive response and thus the corrosion-resistant properties of the vehicle engine Al and Cu metals. It presumed that the METcS inhibitors with electronegative heteroatoms including oxygen-, nitrogen-, sulfur, and the multiple bonded aromatic ring compounds like tinocordiside, isocolumbin, berberine, magnoflorine, *N*-formylannonain, yangambin, 11-hydroxymustakone so on are reported in the literature [61, 62]. Thus, adsorption of these phytoconstituents on the surfaces of the corroded Al and Cu enhances to fabrication of highly stable and less reactive layers, which blocks anodic/cathodic or both sides, and hence prevents significantly the corrosion rates of the metals in the presence of the inhibitors [63]. The degree of such corrosion-preventing layer is mostly in proportionate to the inhibitor concentrations, and it affects the physicochemical characteristics as described above in the adsorption models [64].

Laboratory-based electrochemical methods have been used to look into the corrosion inhibiting behavior of the METcS. The open-circuit potential (OCP) and potentiodynamic polarization measurements were also carried out in this study to know a better understanding of the passivation and stability of the corrosion preventive layers, which formed on the surfaces of Al and Cu metals in BD-100 and BDB-10 fuels without and with METcS concentrations. Figure 3(a) and 3(b) show the changes in the OCP and anodic current density (i_a) of the Al and Cu metals in BD-100 and BDB-10 without and with 500, 1000, 1500, and 2000 ppm METcS at 25±2 °C.

The shifting of the OCP in a noble (more positive) direction and the depletion of the i_a of Al metal is seen with the addition of 500 ppm METcS in the BD-100, while the i_a of Al is increased and shifted the corrosion potential in the less noble direction with the addition of 1000 ppm METcS or more in the BD-100, as noticed on the left-hand side of Figure 3(a). The electrochemical results revealed the fact that the addition of 500 ppm METcS in the BD-100 is enough to inhibit the anodic sides by utilizing an indiscernible adsorption film, which lessens the dissolution reaction of Al metal significantly [65]. Furthermore, additions of 1000-2000 ppm METcS control the corrosion rate of the Al metal in BD-100 by

forming the adsorbed layers on both anodic and cathodic sites, which safeguards further corrosion reactions.

On the other hand, as shown on the right-hand side of Figure 3(a), the i_a of the Cu is increased with METcS additions in BD-100. Besides, the Cu metal shows passive-transpassive dissolution. The dissolution of the passive films formed on the Cu metal could be explained based on the transpassive potential shifting near to the OCP of Cu in pure BD-100 without the METcS inhibitor. The transpassive potential was shifted to the cathodic direction with the addition of 1000 ppm METcS or more in BD-100, as revealed from the anodic polarization curves of the Cu metal. A similar passivation behavior is observed in the anodic polarization curves of the Cu metal in BDB-10 with 500-1500 ppm METcS. Hence, it can be assumed that the METcS functions as a cathodic-anodic inhibitor to enhance the corrosion inhibition efficiency of Al and Cu metals in BD-100, and also the Cu metal in BDB-10.

The cathodic-anodic (i.e., mixed-type) inhibitors are layer-forming compounds that are required to construct an exterior passive layer by hindering both the anodic and cathodic sites of the corroded metals [66]. However, the i_a of Al metal in BDS-10 is usually decreased with increasing the concentrations of the METcS without a remarkable OCP change, as depicted on the left-hand side of Figure 3(b), although the corrosion speed of the Al decreases with the addition of 500-2000 ppm METcS in BDB-10 (Figure 1b). Thereby, the METcS functions as an anodic-type corrosion inhibitor for Al metal even in BDB-10 biofuel.

A comparable consequence of the METcS on the strength and solidity of the anodic passive films of Al and Cu metals is studied in both the BD-100 and BDB-10 biofuels, as shown in Figure 4. A stronger anodic film is formed on both the metals in the 10% biodiesel blend (i.e., BDB-10) than in pure biodiesel (BD-100) in the presence of different concentrations of the plant extract, except 500 ppm METcS for the Al metal, as clearly noticed in Figure 4(a).

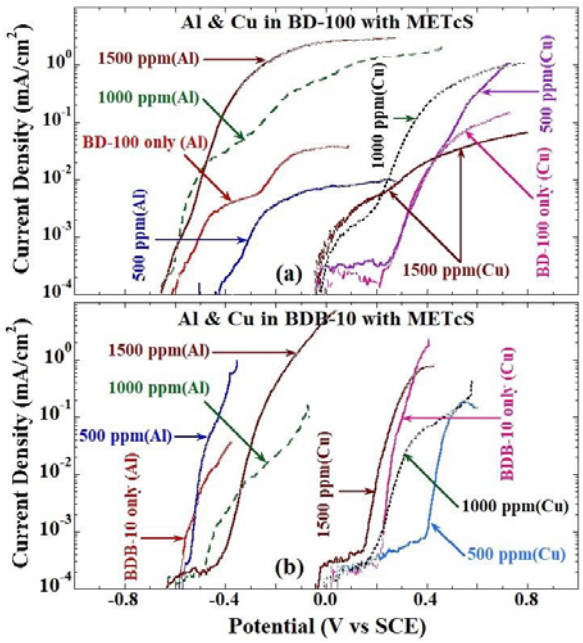

Figure 3. The effects of different concentrations of the METcS inhibitor on the i_a and OCP characteristics of both the Al and Cu metals in (a) BD-100 and (b) BDB-10 at 25±2 °C

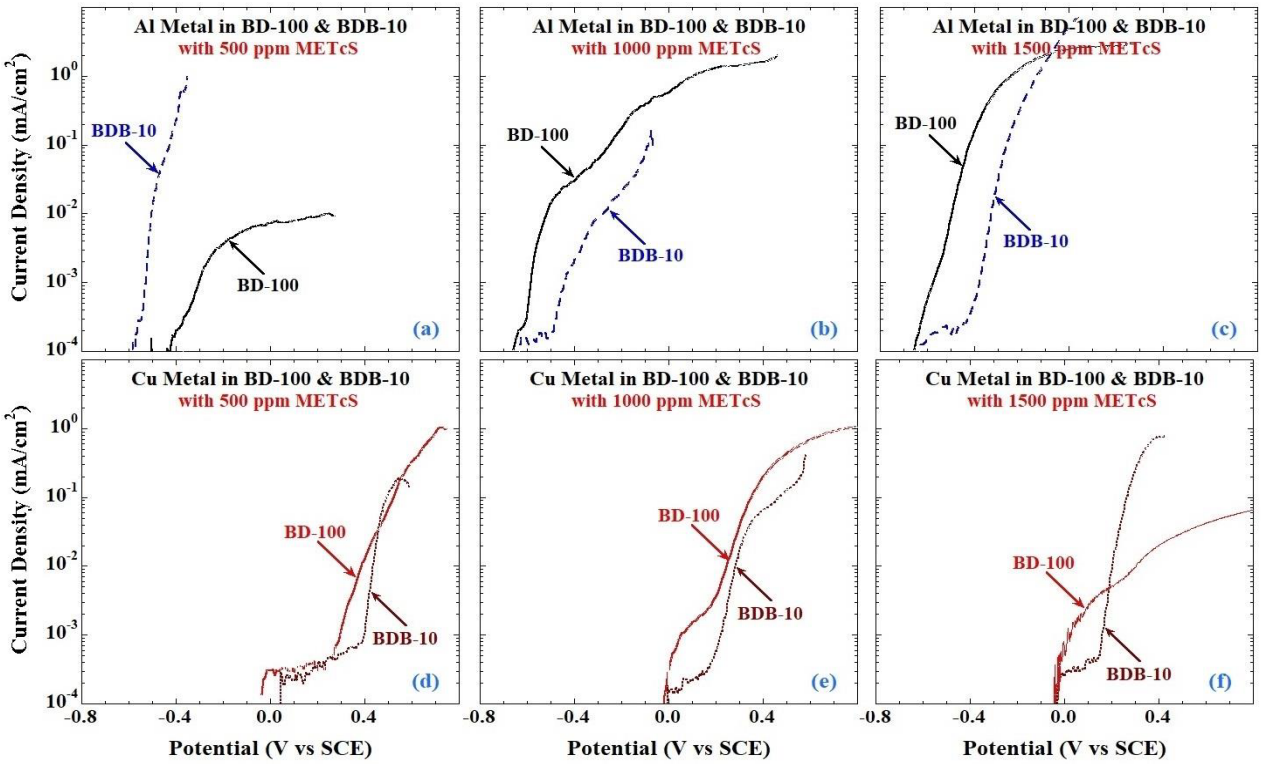

Figure 4. Polarization curves for Al and Cu in B100 and B10 with 500 ppm, 1000 ppm, and 1500 ppm METcS at 25±1 °C in a closed system.

Both the Al and Cu metals show better stability of the anodic passive films formed in the BDB-10 than in BD-100 with different concentrations of the METcS. These results are in close agreement with the experimentally calculated corrosion rate from the weight loss measurement, as discussed above in Figure 1.

4 Conclusions

The anticorrosive effects of the plant-based METcS concentrations for the Al and Cu were reported first time after exposure for more than six months in two varieties of the BDBFs (i.e., BD-100, BDB-10) at 25±2 °C and corked condition, using corrosion, inhibition efficiency, adsorption isotherm, and anodic polarization tests. The novel outcomes of the present work are enumerated as follows;

- The corrosion inhibitory action of the METcS extract on the Al metal increased by increasing its 500-2000 ppm concentrations in BDBFs, although the METcS shows the anomaly behavior to the Cu metal by increasing the concentrations more than 500 ppm BDBFs.
- The outcomes of the electrochemical and corrosion tests suggest the METcS performed as a mixed-type inhibitor for Al and Cu metals in the BDBFs.
- Thermodynamic estimations based on the best fitted Langmuir model alongside the Temkin adsorption models clearly show the adsorption of the majority of METcS phytochemicals on the Al and Cu surfaces without interactions between the METcS phytochemical molecules themselves, which also support the experimental outcomes of the corrosion-resistant and electrochemical polarization tests.
- The results of the adsorption studies also argue for the formation of a corrosion protective layer on the metal surface.
- The green-based METcS could be utilized as a source of biofuel additives on a commercial scale to improve the long-term anticorrosive response of the biodiesel fuels to Al- and Cu-based vehicle engine parts or storage systems.
- More extracts of other plant species can offer as an anticorrosive biofuel additive.

Acknowledgments

This research work was partially supported under the NAST Research Grant No.: 2-2075/76 of Nepal Academy of Science and Technology, Khumaltar, Lalitpur.

References

[1] EU, *Renewable Energy Directive*, (European Commission: Directive 2009/28/EC, revised in 2018) https://energy.ec.europa.eu/topics/renewable-energy/renewable-energy-directive-targets-and-rules/renewable-energy-directive_en (Accessed on 20 June 2022)

[2] D. Singh, D. Sharma, S.L. Soni, S. Sharma, P.K. Sharma, A. Jhalani, A review on feedstocks, production processes, and yield for different generations of biodiesel, *Fuel*, 262 (2020): 116553

[3] B.K. Selvan, S. Das, M. Chandrasekar, R. Girija, S.J. Vennison, N. Jaya, N. Rajamohan, Utilization of biodiesel blended fuel in a diesel engine–combustion engine performance and emission characteristics study, *Fuel*, 311 (2022): 122621

[4] R.R. Kumal, J. Liu, A. Gharpure, R.L. Vander Wal, J.K. Kinsey, B. Giannelli, J.J. Swanson, Impact of biofuel blends on black carbon emissions from a gas turbine engine, *Energy & Fuels*, 34(4) (2020): 4958-4966

[5] S. Dharma, H.C. Ong, H.H. Masjuki, A.H. Sebayang, A.S. Silitonga, An overview of engine durability and compatibility using biodiesel-bioethanol-diesel blends in compression-ignition engines, *Energy Conversion and Management*, 128 (2016): 66-81

[6] H.M. Mahmudul, F.Y. Hagos, R. Mamat, A.A. Adam, W.F.W. Ishak, R. Alenezi, Production, characterization and performance of biodiesel as an alternative fuel in diesel engines – a review, *Renewable and Sustainable Energy Review*, 72 (2017): 497-509

[7] *Biodiesel Benefits and Considerations*, https://afdc.energy.gov/fuels/biodiesel_benefits.html (Accessed on April 3, 2022)

[8] M. Mofijur, F. Kusumo, I.M.R. Fattah, H.M. Mahmudul, M.G. Rasul, A.H. Shamsuddin, T.M.I. Mahlia, Resource recovery from waste coffee grounds using ultrasonic-assisted technology for bioenergy production, *Energies*, 13(7) (2020): 1770

[9] I.S.A. Manaf, N.H. Embong, S.N.M. Khazaai, M.H.A. Rahim, M.M. Yusoff, K.T. Lee, G.P. Maniam, A review for key challenges of the development of biodiesel industry, *Energy Conversion and Management*, 185 (2019): 508-517

[10] P. Katuwal, R. Regmi, S. Joshi, J. Bhattarai, Assessment on the effective green-based Nepal origin plants extract as a corrosion inhibitor for mild steel in bioethanol and its blend, *European Journal of Advanced Chemistry Research*, 15 (2020): 1-13

[11] A. Shehzad, A. Ahmed, M.M. Quazi, M. Jamshaid, S.M. Ashrafur Rahman, M.H. Hassan, H.M.A. Javed, Current research and development status of corrosion behavior of automotive materials in biofuels, *Energies*, 14 (2021): 1440

[12] B.N. Subedi, K. Amgain, S. Joshi, J. Bhattarai, Green approach to corrosion inhibition effect of *Vitex negundo* leaf extract on aluminium and copper metals in biodiesel and its blend, *International Journal of Corrosion and Scale Inhibitor*, 8(3) (2019):744-759

[13] M. Tisza, I. Czinege, Comparative study of the application of steels and aluminium in lightweight production of automotive parts, *International Journal of Lightweight Materials and Manufacture*, 1(4) (2018): 229-238

* Corresponding author: bhattarai_05@yahoo.com

[14] C. Berlanga-Labari, M.V. Biezma-Moraleda, P.J. Rivero, Corrosion of cast aluminum alloys: a review, *Metals,* 10(10) (2020): 1384
[15] S.V. Sajadifar, E. Scharifi, T. Wegener, M. Krochmal, S. Lotz, K. Steinhoff, T. Niendorf, On the low-cycle fatigue behavior of thermo-mechanically processed, high-strength aluminum alloys, *International Journal of Fatigue*, 156 (2022): 106676
[16] M.F.X. Wagner, Light-weight aluminum-based alloys- from fundamental science to engineering applications, *Metals*, 8(4) (2018): 260-264
[17] B. Jones, G. Mead, P. Steevens, M. Timanus, The effect of E20 on metals used in automotive fuel system components, *Report No.: 2-22-2008* (St. Paul, USA: Minnesota Department of Agriculture; 2008).
[18] Y.M. Pusparizkita, A. Harimawan, H. Devianto, T. Setiadi, Effect of bacillus megaterium biofilm and its metabolites at various concentration biodiesel on the corrosion of carbon steel storage tank, *Biointerface Research in Applied Chemistry*, 12(4) (2022): 5698-5708
[19] A. Amaya, O. Piamba, J. Olaya, Corrosiveness of palm biodiesel in gray cast iron coated by thermo-reactive diffusion vanadium carbide coating, *Coatings*, 9(2) (2019): 135
[20] M. Soares, L.O. Berbel, C. Vieira, D.C.S. Oliszeski, C.B. Furstenberger, E.P. Banczek, Study of corrosion of AA 3003 aluminum in biodiesel, diesel, ethanol and gasoline media, *Material Science Forum*, 1012 (2020): 407-411
[21] C.I. Rocabruno-Valdes, J.A. Hernandez, A.U. Juantorena, E.G. Arenas, R. Lopez-Sesenes, V.M. Salinas-Bravo, J.G. Gonzalez-Rodriguez, An electrochemical study of the corrosion behavior of metals in canola biodiesel, *Corrosion Engineering, Science and Technology,* 53(2) (2018): 152-162
[22] L. Longanesi, A.P. Pereira, N. Johnston, C.J. Chuck, Oxidative stability of biodiesel: recent insights, *Biofuels, Bioproducts and Biorefining*, 16(1) (2022): 265-289
[23] M. Somai, A. Giri, A. Roka, J. Bhattarai, Comparative studies on the anti-corrosive action of waterproofing agent and plant extract to steel rebar, *Macromolecular Symposia*, in press (2022).
[24] S. Bouazama, J. Costat, J.M. Desjobertb, A. BenAli, A. Guenbou, M. Tabyaoui, Influence of *Lavandula dentata* essential oil on the corrosion inhibition of carbon steel in 1 M HCl solution, *International Journal of Corrosion and Scale Inhibitor*, 8(1) (2019): 25-41
[25] J. Bhattarai, M. Rana, M.R. Bhattarai, S. Joshi, Effect of green corrosion inhibitor of *Callistemon* plant extract on the corrosion behavior of mild steel in NaCl and HCl solutions, In *Proceedings of CORCON 2016* (Paper No. MI-17, 2016, New Delhi, India: NIGIS/NACE, p. 11)
[26] F.D. Fernandes, L.M. Ferreira, M.L.C.P. da Silva, Application of *Psidium guajava* L leaf extract as a green corrosion inhibitor in biodiesel: biofilm formation and encrustation, *Applied Surface Science Advances*, 6 (2021): 100185
[27] P. Katuwal, K.R. Gaire, J. Bhattarai, Study on the effects of ethylenediamine and plant extract as a corrosion inhibitor for mild steel passivation in bioethanol, In *Proceedings of CORCON-2018* (Paper No. MCI-35, Jaipur, India: NIGIS/ NACE, 2018, p. 9)
[28] R.M. Kunwar, K.P. Shrestha, R.W. Bussmann, Traditional herbal medicine in far West Nepal: a pharmacological appraisal, *Journal of Ethnobiology and Ethnomedicine*, 6 (2010): 35
[29] T. Shrestha, J. Lamichhane, Assessment of phytochemicals, antimicrobial, antioxidant and cytotoxicity activity of methanolic extract of *Tinospora cordifolia* (Gurjo), *Nepal Journal of Biotechnology,* 9(1) (2021): 18-23
[30] M. Rana, S. Joshi, J. Bhattarai, Extract of different plants of Nepalese origin as green corrosion inhibitor for mild steel in 0.5 M NaCl solution, *Asian Journal of Chemistry*, 29(5) (2017): 1130-1134
[31] A. Saxena, D. Prasad, K.K. Thakur, J. Kaur, PDP, EIS, and surface studies of the low-carbon steel by the extract of *Tinospora cordifolia*: a green approach to the corrosion inhibition, *Arabian Journal of Science and Engineering*, 46 (2021): 425-436
[32] M.H. Hussin, M.J. Kassim, N.N. Razali, N.H. Dahon, D. Nasshorudin, The effect of *Tinospora crispa* extracts as a natural mild steel corrosion inhibitor in 1 M HCl solution, *Arabian Journal of Chemistry*, 9 (2016): S616-S624
[33] R. Guzatto, Defferrari D, Reiznautt QB, Cadore IR, Samios D. Trans-esterification double step process modification for ethyl ester biodiesel production from vegetable and waste oil. *Fuel*, 92(1) (2021): 197-203
[34] J. Bhattarai, M. Somai, N. Acharya, A. Giri, A. Roka, N.R. Phulara, Study on the effects of green-based plant extracts and water-proofers as anti-corrosion agents for steel-reinforced concrete slabs, *E3S Web of Conferences*, 302 (2021): 02018
[35] J. Bhattarai, Study on the synergism of corrosion-resistant W-xNb alloys by angle-resolved X-ray photoelectron spectroscopy, *Ceylon Journal of Science*, 50(4) (2021): 513-520
[36] D.B. Pokharel, D.B. Subedi, D. VK, J. Bhattarai, Effects of tungstate and nitrite ions as corrosion inhibitor for Cr-10Zr-10W alloy in 0.5 M NaCl solution, *International Journal of Metal and Alloys*, 5(1) (2019): 11-19
[37] Y.I. Kuznetsov, N.N. Andreev, S.S. Vesely, Why we reject papers with calculations of inhibitor adsorption based on data on protective effects? *International Journal of Corrosion and Scale Inhibitor*, 4(2) (2015): 108-109
[38] I. Langmuir, The constitution and fundamental properties of solids and liquids: part I-Solid, *Journal of the American Chemical Society*, 38(11) (1916): 2221-2295

[39] M.I. Temkin, Adsorption equilibrium and the kinetics of processes on non-homogeneous surfaces and in the interaction between adsorbed molecules, *Zhurnal Fiziche-Skoi Khimii*, 15 (1941): 296-332
[40] F.T. Kamga, Modeling adsorption mechanism of paraquat onto Ayous (*Triplochiton scleroxylon*) wood sawdust, *Applied Water Science*, 9 (2019): 1
[41] D.B. Subedi, D.B. Pokharel, J. Bhattarai, Assessment on the effects of sodium salts of tungstate and nitrite as green inhibitor for the corrosion of Cr–5Ni–53W alloy in 0.5 M NaCl solution*, International Journal of Metallurgy and Alloys,* 6(1) (2020): 25-36
[42] M.A. Deyab, Corrosion inhibition of aluminum in biodiesel by ethanol extracts of Rosemary leaves, *Journal of the Taiwan Institute of Chemical Engineers*, 58 (2016): 536-541
[43] ASTM D6751-14, *Standard specification for biodiesel fuel blend stock (B100) for middle distillate fuels* (West Conshohocken, USA: ASTM International, 2014)
[44] C.R. Whetstine, GC-MS analysis of synthesized biodiesel, In *Forensic Science Master's Projects-1*, 2020
[45] A.S. Luna, A.P. Da Silva, J. Ferre, R. Boque, Classification of edible oils and modeling of their physico-chemical properties by chemometric methods using mid-IR spectroscopy, *Spectrochimi Acta A: Molecular and Biomolecular Spectroscopy*, 100 (2013): 109-114
[46] A.S. Silitonga, A.H. Shamsuddin, T.M.I. Mahlia, J. Milano, F. Kusumo, J. Siswantoro, … H.C. Ong, Biodiesel synthesis from *Ceiba pentandra* oil by microwave irradiation-assisted transesterification: ELM modeling and optimization, *Renewable Energy*, 146 (2020): 1278-1291
[47] A.S. Luna, J.S. de Gois, Application of chemometric methods coupled with vibrational spectroscopy for the discrimination of plant cultivars and to predict physicochemical properties using R, *Comprehensive Analytical Chemistry*, 80 (2018): 165-194
[48] J.Y. Chen, H. Zhang, J. Ma, T. Tuchiya, Y. Miao, Determination of the degree of degradation of frying rapeseed oil using Fourier-transform infrared spectroscopy combined with partial least-squares regression, *International Journal of Analytical Chemistry*, 2015 (2015): 185367
[49] A.T. Hoang, M. Tabatabaei, M. Aghbashlo, A review of the effect of biodiesel on the corrosion behavior of metals/alloys in diesel engines, *Energy Sources Part A: Recovery, Utilization, and Environmental Effects*, 42(23) (2020): 2923-2943
[50] M. Fazal, A. Haseeb, H. Masjuki, Degradation of automotive materials in palm biodiesel, *Energy*, 40(1) (2012): 76-83
[51] C.L. Kugelmeier, M.R. Monteiro, R. da Silva, S.E. Kuri, V.L. Sordi, C.A. Della Rovere, Corrosion behavior of carbon steel, stainless steel, aluminum and copper upon exposure to biodiesel blended with petrodiesel, *Energy*, 226 (2021): 120344
[52] A. Devi, V.K. Das, D. Deka, Ginger extract as a nature-based robust additive and its influence on the oxidation stability of biodiesel synthesized from non-edible oil, *Fuel*, 187 (2017): 306-314
[53] M. Mobin, I. Ahmad, M. Basik, M. Murmu, P. Banerjee, Experimental and theoretical assessment of almond gum as an economically and environmentally viable corrosion inhibitor for mild steel in 1 M HCl, *Sustainable Chemistry and Pharmacy*, 18 (2020): 100337
[54] M.N. Al-Ghouti, D.A. Da'ana, Guidelines for the use and interpretation of adsorption isotherm models: a review, *Journal of Hazardous Materials*, 393 (2020): 122383
[55] N. Ayawei, A.N. Ebelegi, D. Wankasi, Modelling and interpretation of adsorption isotherms, *Journal of Chemistry*, 2017 (2017):3039817
[56] P. Magrati, D.B. Subedi, D.B. Pokharel, J. Bhattarai, Appraisal of different inorganic inhibitors action on the corrosion control mechanism of mild steel in HNO_3 solution, *Journal of Nepal Chemical Society*, 41(1) (2020): 64-73
[57] D. Vk, J. Bhattarai, Effect of sodium tungstate as a green corrosion inhibitor on the passivation behavior of mild steel in aggressive media, *International Journal of Applied Science and Biotechnology*, 4(2) (2016): 183-190
[58] F. Batool, J. Akbar, S. Iqbal, S. Noreen, S.N.A. Bukhari, Study of isothermal, kinetic, and thermodynamic parameters for adsorption of cadmium: An overview of linear and nonlinear approach and error analysis, *Bioinorganic Chemistry and Applications*, 2018 (2018): 3463724
[59] S.L. Lam, R. Ballinger, C. Forsberg, Modeling and predicting total hydrogen adsorption in nanoporous carbon materials for advanced nuclear systems, *Journal of Nuclear Materials*, 511 (2018): 328-340
[60] C. Aharoni, M. Ungarish, Kinetics of activated chemisorption Part 2: theoretical models, *Journal of the Chemical Society, Faraday Transactions 1: Physical Chemistry in Condensed Phases*, 73 (1977): 456-464
[61] V. Sagar, A.H.S. Kumar, Efficacy of natural compounds from *Tinospora cordifolia* against SARS-CoV-2 protease, surface glycoprotein and RNA polymerase, *Biology, Engineering, Medicine and Science Reports*, 6(1) (2020): 6-8
[62] E. Okon, W. Kukula-Koch, A. Jarzab, M. Halasa, A. Stepulak, A. Wawruszak, Advances in chemistry and bioactivity of magnoflorine and magnoflorine-containing extracts, *International Journal of Molecular Sciences*, 21(4) (2020): 1330
[63] T.J. Harvey, F.C. Walsh, A.H. Nahle, A review of inhibitors for the corrosion of transition metals in aqueous acids, *Journal of Molecular Liquids*, 266 (2018): 160-175
[64] D.B. Pokharel, D.B. Subedi, J. Bhattarai, Study the effect of sodium nitrite as a green inhibitor for the sputter-deposited tungsten-based ternary alloys in 0.5 M NaCl solution, *Bibechana* 12 (2015): 1-12
[65] I.A.W. Ma, S. Ammar, S.S.A. Kumar, K. Ramesh, S. Ramesh, A concise review on corrosion inhibitors: types, mechanisms and electrochemical

evaluation studies, *Journal of Coating Technology and Research*, 19 (2022): 241-268

[66] D.B. Subedi, D.B. Pokharel, J. Bhattarai, Study the corrosion inhibition mechanism of sputter-deposited W-42Cr-5Ni and Cr-10Zr-10W alloys by sodium nitrite as a green inhibitor in 0.5 M NaCl and 1 M NaOH solutions, *International Journal of Applied Science and Biotechnology,* 2(4) (2014): 537-543

* Corresponding author: bhattarai_05@yahoo.com